01,11

Surface crystallization of amorphous $Fe_{73.8}Si_{13}B_{9.1}Cu_1Nb_{3.1}$ and $Fe_{77.5}Si_{13.5}B_9$ microwires

© A.A. Fuks[1,2], G.E. Abrosimova[1], O.I. Aksenov[1], A.S. Aronin[1]

[1] Osipyan Institute of Solid State Physics RAS,
Chernogolovka, Russia
[2] HSE University,
Moscow, Russia

E-mail: artemfux@yandex.ru

Received October 7, 2022
Revised October 7, 2022
Accepted October 19, 2022

Amorphous microwires of $Fe_{73.8}Si_{13}B_{9.1}Cu_1Nb_{3.1}$ and $Fe_{77.5}Si_{13.5}B_9$ composition fabricated by the Ulitovsky–Taylor method were studied. The samples with the glass shell removed were heated at temperatures of 753 K and 703 K for 20 min, afterwards, their structure was examined using X-ray diffraction. Subsequently, the thermally treated samples were chemically etched and X-ray diffraction study of the structure was again carried out. Experimental results on the predominant crystallization of near-surface regions were discussed assuming that mechanical stresses affect the nucleation and growth of nanocrystals.

Keywords: amorphous materials, stress distribution, nanocrystallization, X-ray diffraction.

DOI: 10.21883/PSS.2023.01.54970.494

1. Introduction

Amorphous-nanocrystalline materials obtained by heat treatment of amorphous iron-based alloys are well known for their magnetic properties, combining high values of magnetic permeability and saturation magnetization with low magnetostriction and low losses on remagnetization [1–4]. The Ternary alloys of the Fe-Si-B system, as well as Fe-Si-B alloys with the addition of other elements, in particular, Cu and Nb, are quite indicative here. The best magnetic characteristics of these alloys from the point of view of practical application are obtained when a two-phase state is reached: nanocrystals of a solid solution of silicon in BCC-iron α-Fe(Si) with an average size of 10−20 nm, distributed in the remaining amorphous matrix. The main mechanism of formation of nanocrystals in Fe-Si-B alloys during heat treatment is — homogeneous nucleation. The addition of Cu to the alloy leads to the precipitation of copper clusters that contribute to the formation of nanocrystals and act as centers of heterogeneous nucleation. In turn, Nb slows down the growth of nanocrystals and the formation of iron borides [5]. Amorphous microwires in a glass shell from these alloys can be made by the Ulitovsky–Taylor method. During the manufacturing process, the melt in the glass shell undergoes a sharp cooling, which leads to the formation of an amorphous structure. The large temperature gradient and the difference in the coefficients of thermal expansion between the metal core of the microwires and the glass shell determine the magnitude and nature of the distribution of internal stresses. The solution of the thermal conductivity equation performed in [6] showed that tensile axial stresses predominate in the central part of the microwire, and in the near-surface region — strong compressive axial stresses (of the order of GPa units). At the same time, removing the shell does not change the nature of the stress distribution, but only lowers the overall level by several hundred MPa. Therefore, the purpose of this work is to evaluate the effect of strong compressive stresses on the kinetics of crystallization and to experimentally verify this effect on the example of amorphous microwires of the composition $Fe_{73.8}Si_{13}B_{9.1}Cu_1Nb_{3.1}$ and $Fe_{77.5}Si_{13.5}B_9$.

2. Materials and research methods

Amorphous microwires in a glass shell made of $Fe_{73.8}Si_{13}B_{9.1}Cu_1Nb_{3.1}$ and $Fe_{77.5}Si_{13.5}B_9$ were obtained by the Ulitovsky–Taylor method, the average diameter of the metal part is 16.5 μm, the thickness of the shell — 3.5 μm. The microwires with the removed shell were annealed in vacuum at a temperature of 753 and 703 K for 20 min. The removal of the glass shell was carried out by chemical etching in hydrofluoric acid, the removal of the surface layer was carried out in a mixture of hydrofluoric and nitric acids.

The structure and phase composition of the samples before and after annealing were studied. on a SIEMENS D-500 diffractometer using CoK_α-radiation. Since the samples contained amorphous and crystalline phases, the experimental curves were decomposed into a diffuse component due to scattering from the amorphous phase and a diffraction component due to the presence of crystals. When decomposing, the characteristics of the scattering curve by the initial amorphous phase (half-width, position of the diffuse maximum) were taken into account. The size of the nanocrystals was calculated from the half-width of the

diffraction component of the spectrum using the Scherrer formula [7]. The fraction of the crystalline and amorphous phases was estimated by the ratio of the integral intensities of the diffraction and diffuse components of the diffraction pattern in accordance with [8].

3. Results and discussion

The samples after manufacturing were amorphous. The amorphous structure of both samples changes markedly during heat treatment. According to the works [9,10], crystallization of alloys $Fe_{73.8}Si_{13}B_{9.1}Cu_1Nb_{3.1}$ and $Fe_{77.5}Si_{13.5}B_9$ begins at a temperature of approximately 753 and 703 K, respectively, therefore, such temperatures were chosen to study the early stages of crystallization. The distribution of the initial stresses has the form described in [6]. In the central part of the microwires, tensile axial stresses mainly act, the near-surface area is exposed mainly to compressive axial stresses reaching units of GPa. The removal of the glass shell does not change the nature of the stress distribution, but lowers the overall stress level in the micro-wire by several hundred MPa.

Figures 1 and 2 show diffraction patterns of microwires of the composition $Fe_{73.8}Si_{13}B_{9.1}Cu_1Nb_{3.1}$ and $Fe_{77.5}Si_{13.5}B_9$ with the shell removed before (a) and after (b) chemical etching of the metal surface annealed at a temperature of 753 and 703 K for 20 min.

Both figures show the regions of the main maximum; the curve *1* is an experimental diffraction pattern, the curve *3* corresponds to amorphous phase scattering, the curve *4* describes diffraction reflections from nanocrystals, the curve *2* is the sum of the curves *3* and *4*. Diffraction reflections from the nanocrystalline phase, which correspond to the phase with the BCC lattice of the Fe(Si) solid solution, are observed on the X-ray diffraction patterns of the microwires of both compositions. The analysis of the reflection intensities showed that the volume fraction of nanocrystals in the microwires of both compositions is several percent. On the diffraction patterns of microwires after removal of near-surface areas by chemical etching (Fig. 1, 2, b) there are no diffraction reflections, only wide diffuse maxima are present. Thus, it can be concluded that crystallization under the selected heat treatment conditions occurred mainly at the surface of the microwires.

The experimental results obtained are explicable from the point of view of the influence of mechanical stresses on the nucleation and growth of crystals. Taking into account the elastic energy of deformation resulting from high-speed cooling of the melt, we write down expressions for the rates of nucleation I and growth of nanocrystals u_c [11,12]:

$$I = DN_V \exp\left(-16\pi\sigma^3/3kT[\Delta G_{\text{ch}} + E_\varepsilon]^2\right)/a_0^2, \quad (1)$$

$$u_c = fD\left[1 - \exp(-(\Delta G_{\text{ch}} + E_\varepsilon)/kT)\right]/a_0, \quad (2)$$

where D — diffusion coefficient, a_0 — average interatomic distance, N_V — average atomic concentration, $f \sim 1$ — dimensionless factor, G_{ch} — the driving force of crystallization from the amorphous state. Elastic energy E_ε — is proportional to the square of the deformation

$$\varepsilon(r) = \Delta V/3V + \gamma\sigma(r)/E, \quad (3)$$

where $\Delta V/3V$ — volumetric crystallization effect, $\sigma(r)$ — sum of diagonal components of the stress tensor, E — Young's modulus. To account for stress relaxation during heat treatment, a numerical factor γ was introduced, meaning the proportion of stresses remaining after heat treatment. According to [13], the density of the amorphous alloy $Fe_{73.5}Si_{13.5}B_9Cu_1Nb_3$ is $7.14 \cdot 10^3$ kg/m^3, density of amorphous alloy $Fe_{77.5}Si_{13.5}B_9$ — $7.20 \cdot 10^3$ kg/m^3 [6], the density of nanocrystals of a solid solution of 25% silicon

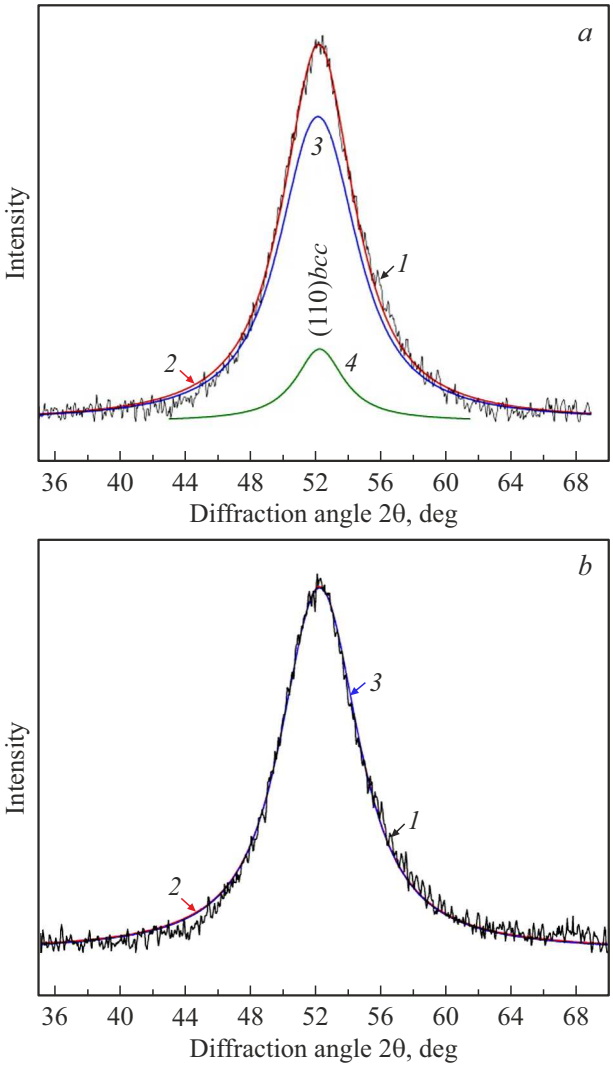

Figure 1. Diffraction patterns of microwires of the composition $Fe_{73.8}Si_{13}B_{9.1}Cu_1Nb_{3.1}$ with the shell removed before (a) and after (b) chemical etching of the metal core annealed at temperature $T_{\text{ann}} = 753$ K for 20 min (*1* — experimental curve, *2* — summary curve, *3* — scattering from amorphous phase, *4* — diffraction reflections from nanocrystals).

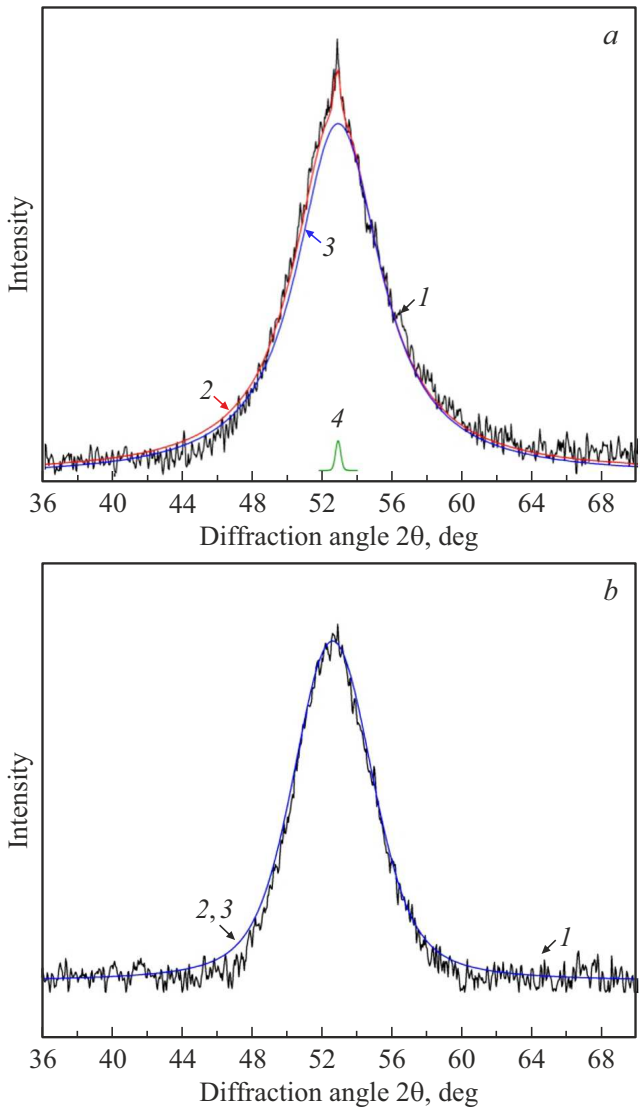

Figure 2. Diffraction patterns of microwires of the composition $Fe_{77.5}Si_{13.5}B_9$ with the removed shell before (*a*) and after (*b*) chemical etching of the metal core, annealed at temperature $T_{ann} = 753$ K for 20 min (*1* — experimental curve, *2* — total curve, *3* — scattering from amorphous phase).

in iron Fe_3Si is $7.39 \cdot 10^3$ kg/m^3 [14], the density of iron is $7.87 \cdot 10^3$ kg/m^3. Assuming that the density changes linearly with the change in Si concentration, the density of nanocrystals was assumed to be $7.55 \cdot 10^3$ kg/m^3 with a Si content of 16.5% [15]. The volume effect during the formation of crystals in an amorphous matrix is negative and for the alloy $Fe_{73.5}Si_{13.5}B_9Cu_1Nb_3$ is equal to -5.7%, for alloy $Fe_{77.5}Si_{13.5}B_9$ — -4.9%. Based on the distribution of the components of the internal stress tensor calculated according to the work [6], the elastic energy takes maximum values in the near-surface region of the microwire, where compressive axial stresses dominate. Since the volumetric effect of crystal formation is negative, the rates of crystal nucleation and growth will increase in this region (expressions (1) and (2)). This, in turn, will lead to an increase in the proportion of the nanocrystalline phase in the near-surface region of the microwire, which, according to [16], is written in form

$$X = 1 - \exp(-\pi I u_c^3 t^4/3), \qquad (4)$$

where t — heat treatment time. Calculated by (4) fractions of the nanocrystalline phase in $Fe_{73.8}Si_{13}B_{9.1}Cu_1Nb_{3.1}$ and $Fe_{77.5}Si_{13.5}B_9$ for different values of the parameter γ are shown in Fig. 3.

As follows from the theoretical estimate, the crystallization of microwires of the composition $Fe_{73.8}Si_{13}B_{9.1}Cu_1Nb_{3.1}$ and $Fe_{77.5}Si_{13.5}B_9$ begins in the near-surface region where large compressive stresses are present. The value of the parameter γ, which characterizes the stress level, at the same time changes only the total volume fraction of nanocrystals, which decreases with a decrease of γ. The experimental results obtained for the approximate fraction of nanocrystals of several percent correspond to the value of $\gamma = 0.1$. A change in the

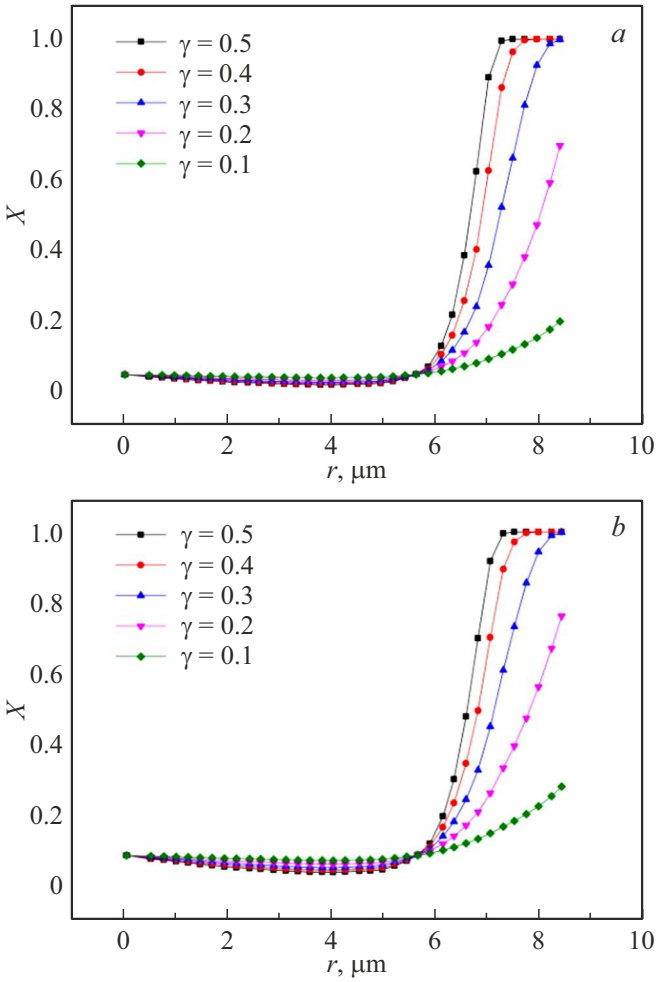

Figure 3. Volume fraction of nanocrystals in the alloy *a* — $Fe_{73.8}Si_{13}B_{9.1}Cu_1Nb_{3.1}$ ($T_{ann} = 753$ K) and *b* — $Fe_{77.5}Si_{13.5}B_9$ ($T_{ann} = 703$ K) at different values of the parameter γ after heat treatment for 20 min.

kinetics of crystallization of amorphous alloys under the action of mechanical stresses was observed earlier in the work [17]. Curved ribbon made of amorphous alloy $Pd_{40}Cu_{30}Ni_{10}P_{20}$ was crystallized at a temperature of 700 K. Since the volumetric effect during the separation of Cu_3Pd nanocrystals was negative and amounted to -2%, an acceleration of crystallization in the compressed regions of the tape was expected, which was achieved. At the same time, no nanocrystals were found in the stretched areas of the tape. In the iron-based alloys studied by us in this work, the volume effect of crystallization is larger in magnitude, and its effect on the crystallization process should be more significant.

As we have already mentioned, it was found that in microwires made of $Fe_{73.8}Si_{13}B_{9.1}Cu_1Nb_{3.1}$ and $Fe_{77.5}Si_{13.5}B_9$ crystallization at the initial stages occurs at the surface; the central part of the microwires remains amorphous. Thus, the improvement of the magnetic properties of the material associated with the formation of nanocrystals should also occur mainly at the surface of the microwires, which may allow consciously influencing the high-frequency magnetic properties of the microwires, for example, the effect of a giant magnetic impedance.

4. Conclusion

As a result, it was established:

1. Crystallization of microwires of the composition $Fe_{73.8}Si_{13}B_{9.1}Cu_1Nb_{3.1}$ and $Fe_{77.5}Si_{13.5}B_9$ starts in the near-surface regions. The inhomogenous distribution of crystals over the cross-section of microwires is due to the dependence of the rates of nucleation and growth on the level and type of mechanical stresses.

2. The possibility of forming a near-surface nanocrystalline layer in microwires opens up new opportunities for the formation of materials with enhanced magnetic properties.

Funding

The work was supported by the Russian Science Foundation (project No. 22-72-00067).

Conflict of interest

The authors declare that they have no conflict of interest.

References

[1] Nanocrystalline Soft Magnetic Material FINEMET. [Electronic resource] // Hitachi Metals, Ltd. URL: https://www.hitachi-metals.co.jp/e/products/elec/tel/p02_21.html (date of access 09.20.2022)
[2] G. Herzer. Phys. Scripta **1993**, *T49A*, 307 (1993).
[3] N.V. Ershov, Yu.P. Chernenkov, V.A. Lukshina, O.P. Smirnov, D.A. Shishkin. FTT **63**, *7*, 834 (2021). (in Russian).
[4] O.I. Aksenov, A.S. Aronin. FTT **63**, *4*, 513 (2021).
[5] S. Kaloshkin, M. Churyukanova, V. Zadorozhnyi, I. Shchetinin, R.K. Roy. J. Alloys Compd. **509**, *Suppl. 1*, S400 (2011).
[6] H. Chiriac, T.A. Óvári, G. Pop. Phys. Rev. B **52**, *14*, 10104 (1995).
[7] A. Guinier. Theorie et technique de la radiocristallographie. Dumond, Paris (1956).
[8] G.E. Abrosimova, A.S. Aronin, N.N. Kholstinina. FTT **52**, *3*, 417 (2010). (in Russian).
[9] W.Z. Chen, P.L. Ryder. Mater. Sci. Eng. B **34**, *2–3*, 204 (1995).
[10] A. Inoue, T. Masumoto, M. Kikuchi, T. Minemura. J. Jpn Inst. Met. Mater. **42**, 294 (1978).
[11] N. Nishiyama, A. Inoue. Acta Mater. **47**, *5*, 1487 (1999).
[12] D.R. Uhlmann. J. Non-Cryst. Solids **7**, *4*, 337 (1972).
[13] R. Parsons, K. Ono, Z. Li, H. Kishimoto, T. Shoji, A. Kato, M.R. Hill, K. Suzuki. J. Alloys Compd. **859**, 157845 (2021).
[14] Materials Data on Fe3Si. K. Persson (SG: 225) [Electronic resource]. Materials Project, 2016. URL: https://materialsproject.org/materials/mp-2199/ (date of access 09.19.2022)
[15] T. Gheiratmand, H.R. Madaah Hosseini. J. Magn. Magn. Mater. **408**, 177 (2016).
[16] J.W. Christian. The Theory of Phase Transformations in Metals and Alloys. Pergamon Press, Oxford (1965).
[17] A.R. Yavari, K. Georgarakis, J. Antonowicz, M. Stoica, N. Nishiyama, G. Vaughan, M. Chen, M. Pons. Phys. Rev. Lett. **109**, *8*, 085501 (2012).